autocrine growth stimulation (*1, 3*). When EBV-immortalized cells are cultured at high densities, there are high concentrations of such factors, and cell growth cannot be enhanced further. However, when they are cultured at low cell densities, cell growth becomes dependent on exogenous factors, including IFN-β_2/BSF-2. This requirement that the cells be cultured at low density for the growth-promoting effects of IFN-β_2/BSF-2 to be observed may explain why this effect has not been documented previously (*9*).

We do not know whether this growth factor is B cell lineage–specific, whether it is selective for B cells activated by EBV, or whether it is part of a network of cytokine interactions. We report here that IFN-β_2/BSF-2/IL-6 is a potent growth factor for human B cells infected with EBV. This newly described property of the molecule emphasizes its role as an important mediator of the immune response in humans.

REFERENCES AND NOTES

1. B. A. Blazar, L. M. Sutton, M. Strome, *Cancer Res.* **43**, 4562 (1983); J. Gordon, S. C. Ley, M. D. Melamed, P. Aman, N. C. Hughes-Jones, *J. Exp. Med.* **159**, 1554 (1984).
2. G. Tosato and S. Pike, *Fed. Proc. Fed. Am. Soc. Exp. Biol.* **46**, 2707 (1987); G. Tosato, N. Goldman, T. C. Gerrard, S. E. Pike, in preparation.
3. J. Gordon, S. C. Ley, M. D. Melamed, L. S. English, N. C. Hughes-Jones, *Nature (London)* **310**, 145 (1984).
4. J. Gordon, G. Guy, L. Walker, *Immunology* **57**, 419 (1986); L. Rimsky *et al.*, *J. Immunol.* **136**, 3304 (1986); G. Scala *et al.*, *ibid.* **138**, 2527 (1987); H. Wakasugi *et al.*, *Proc. Natl. Acad. Sci. U.S.A.* **84**, 804 (1987).
5. G. Tosato, K. B. Seamon, K. D. Jones, S. Pike, in preparation. Briefly, the purification was accomplished by sequential cation-exchange chromatography over CM-Sephadex, anion-exchange chromatography over DEAE-Sephacel, and reversed-phase high-performance liquid chromatography over a Synchropak RP-P C_{18} column. Recovery of activity at each purification step was monitored by testing the proliferation of an indicator lymphoblastoid cell line.
6. U. K. Laemmli, *Nature (London)* **227**, 680 (1970).
7. B. R. Oakley, D. R. Kirsch, N. R. Morris, *Anal. Biochem.* **105**, 361 (1980).
8. J. Weissenbach *et al.*, *Proc. Natl. Acad. Sci. U.S.A.* **77**, 7152 (1980); P. B. Sehgal and A. D. Sagar, *Nature (London)* **288**, 95 (1980); A. Zilberstein, R. Ruggieri, J. H. Korn, M. Revel, *EMBO J.* **5**, 2529 (1986); L. T. May, D. C. Helfgott, P. B. Sehgal, *Proc. Natl. Acad. Sci. U.S.A.* **83**, 8957 (1986).
9. T. Hirano *et al.*, *Proc. Natl. Acad. Sci. U.S.A.* **82**, 5490 (1985); T. Hirano *et al.*, *ibid.* **84**, 228 (1987); T. Hirano *et al.*, *Nature (London)* **324**, 73 (1986).
10. L. T. May *et al.*, in preparation.
11. M. Kohase, D. Henriksen-DeStafano, L. T. May, J. Vilček, P. B. Sehgal, *Cell* **45**, 659 (1986).
12. For a review, see P. B. Sehgal, L. T. May, I. Tamm, J. Vilček, *Science* **235**, 731 (1987); A. Billiau, *Immunol. Today* **8**, 84 (1987).
13. J. Content *et al*, *Proc. Natl. Acad. Sci. U.S.A.* **79**, 2768 (1982); P. Poupart *et al.*, *EMBO J.* **6**, 1219 (1987); G. Haegeman *et al.*, *Eur. J. Biochem.* **159**, 652 (1986).
14. J. Van Damme *et al.*, *J. Exp. Med.* **165**, 914 (1987).
15. J. Gauldie, C. Richards, D. Harnish, P. Lansdorp, H. Baumann, *Proc. Natl. Acad. Sci. U.S.A.* **84**, 7251 (1987); M. W. N. Nijsten *et al.*, *Lancet* **1987-II**, 921 (1987).
16. G. H. W. Wong and D. V. Goeddel, *Nature (London)* **323**, 819 (1986).
17. C. Vaquero, J. Sanceau, J. Weissenbach, F. Beranger, R. Falcott, *J. Interferon Res.* **6**, 161 (1986).
18. P. K. Smith *et al.*, *Anal. Biochem.* **150**, 76 (1985).

19. We thank T. Hirano and T. Kishimoto for recombinant BSF-2; J. Vilček for providing antiserum to IFN-β; M. Moos, D. Morris, J. Robbins, and J. Regan for technical help; and R. Yarchoan for revising the manuscript. Supported in part by USPHS grants AI-16262 and CA-44365 (L.T.M. and P.B.S.), by a contract from the National Foundation for Cancer Research, and by an established investigatorship award from the American Heart Association (P.B.S.).

1 September 1987; accepted 4 December 1987

The Effect of Eurasian Snow Cover on Global Climate

T. P. Barnett, L. Dümenil, U. Schlese, E. Roeckner

Numerical simulations with a global atmospheric circulation model suggest that large-scale variations in the amount of snowfall over Eurasia in the springtime are linked to the subsequent strength of the Asian summer monsoon. Large-scale changes in Eurasian snow cover are coupled to larger scale changes in the global climate system. There is a large, strong teleconnection to the atmospheric field over North America. The model results also show snow cover effects to subsequently alter other climatic fields known to be intimately associated with the El Niño–Southern Oscillation (ENSO) phenomenon. Thus the model results seem to challenge the current dogma that the ENSO phenomenon is solely the result of close coupling between the atmosphere and ocean by suggesting that processes over continental land masses may also have to be considered.

Over 100 years ago, Henry Blanford (*1*) hypothesized that unusually heavy snow in the Himalayas preceded a failure of the Indian summer monsoon, and that this regional effect might be part of a "larger scale" climatic change associated with large-scale changes in snow cover over Eurasia. Recently, other researchers have argued also for the potential importance of the possible role of Eurasian snow cover in global climate dynamics (*2*), but only in the last decade has a serious effort been made to check such hypotheses (*3–6*). Unfortunately, studies conducted to date have been largely empirical and have yielded results that, while supportive of the original ideas, are largely unconvincing because of data problems or other limitations.

We have conducted simulations with a global general circulation model (GCM) in which the snow depth over the Eurasian continent was varied from its climatological norm and the subsequent climatic changes in the model noted. In simulations where the snow amount is increased, the model's summer monsoon is characterized by less rainfall, higher surface pressure over Southeast Asia, and reduced winds over the Arabian Sea (Fig. 1). These climatic changes are generally associated with a poor monsoon. The model simulations also suggest that the failure of the Asian monsoon is, as Blanford guessed, part of a far larger modulation of the global climate system. Specifically, there appear to be important teleconnections between the large convection region of Southeast Asia and the atmospheric fields over the tropical Pacific and North America (Figs. 2 and 3). These results all strongly support the original hypothesis that the amount of snow on the Eurasian continent in the spring has an important subsequent impact on both regional and global climate variations.

The physics responsible for the above results in the GCM are generally complex. The regional effects include all elements of the surface heat budget and the soil hydrology. The presence of the snow, its melting, and evaporation of its melt water retard and diminish warming of the Asian land mass and subsequent establishment of the land-sea temperature contrast that drives the monsoon circulation. The reason for the remote teleconnection to North America involves large-scale thermal forcing over the Asian land mass and subsequent adjustment, via Rossby wave dynamics, of the ultralong wave structure of the atmosphere. The tropical response is due to direct thermal forcing associated with the latent heat release during monsoon precipitation anomalies.

The details of our experiments were as follows. The model we used was a version of

T. P. Barnett, Climate Research Group, Scripps Institution of Oceanography, La Jolla, CA 92093.
L. Dümenil, U. Schlese, E. Roeckner, Meteorologisches Institüt, University of Hamburg, Bundestrasse 55, 2000 Hamburg 13, West Germany.

the European Centre for Medium Range Weather Forecasts (ECMWF) forecast model used for climate simulations at Hamburg University (*7*). This global model with T21 spectral truncation has a fully interactive hydrological cycle. It was forced with observed seasonal variations in sea surface temperature, solar angle, and so forth. A 10-year control run (C) provided a backdrop against which to gauge the significance of our perturbation experiments. The control run showed that the model is capable of reproducing surprisingly well both the observed winter-spring snow field over Eurasia and the observed summer monsoon conditions (geopotential height, surface wind, and precipitation fields) over Southeast Asia. Thus there is good reason to believe the perturbation experiments are representative of the real world situations.

A set of four perturbation experiments (D) began from four different 1 January initial atmospheric states given by the control run. The integrations were continued through September. All forcing in D was identical to C except that the amount of the snow laid down over Eurasia was doubled. A second set of four perturbation experiments (H) was run with the snowfall over Eurasia being reduced by one half. Snow depths in no other part of the world were altered nor were any of the other forcing fields. The actual snowfall rate was doubled (or halved) after it was computed in the model. This ensured that the model energetics were not perturbed by the experimental procedure. The differences in snow depth between D and H experiments and C seemed reasonable, for example, on average over the snow-covered regions of Eurasia, D had 10.7 cm (water equivalent) more snow than C in June, whereas H had typically 1.6 cm less.

The results of the experiments given below are often expressed as the difference between the D or H experiments minus the control run; this difference being divided by the standard deviation σ obtained from the 10-year control run, for example, $(D - C)/\sigma$. This is a t statistic and values greater than 1.83 and 2.26 indicate that the grid point values in the D and C realizations are different from each other at the 0.10 and 0.05 significance level, respectively. However, statistical significance statements are based on application of a more powerful, nonparametric permutation procedure (PPP) to the GCM data sets (*8*).

Results for June represent well our numerical experiments (Fig. 1). During the increased snow depth (D) experiment, sea level pressure (SLP) over much of Asia is higher by 2 to 8 mbar than during the control run (Fig. 1A). The difference agrees well with observed SLP differences between poor and normal monsoon seasons. For increased snow depth, the temperature in the atmospheric column from surface (Fig. 1B) to at least 200 mbar averaged over Asia is colder by 1.7° to 3.6°C than normal, as is the deep soil temperature. Observations from upper air stations in the region show temperature differences in the atmospheric column that are 2° to 3°C colder during poor monsoons relative to long-term norms; again, a good correspondence. Since the Indian Ocean's surface temperature changes little, the land-sea temperature con-

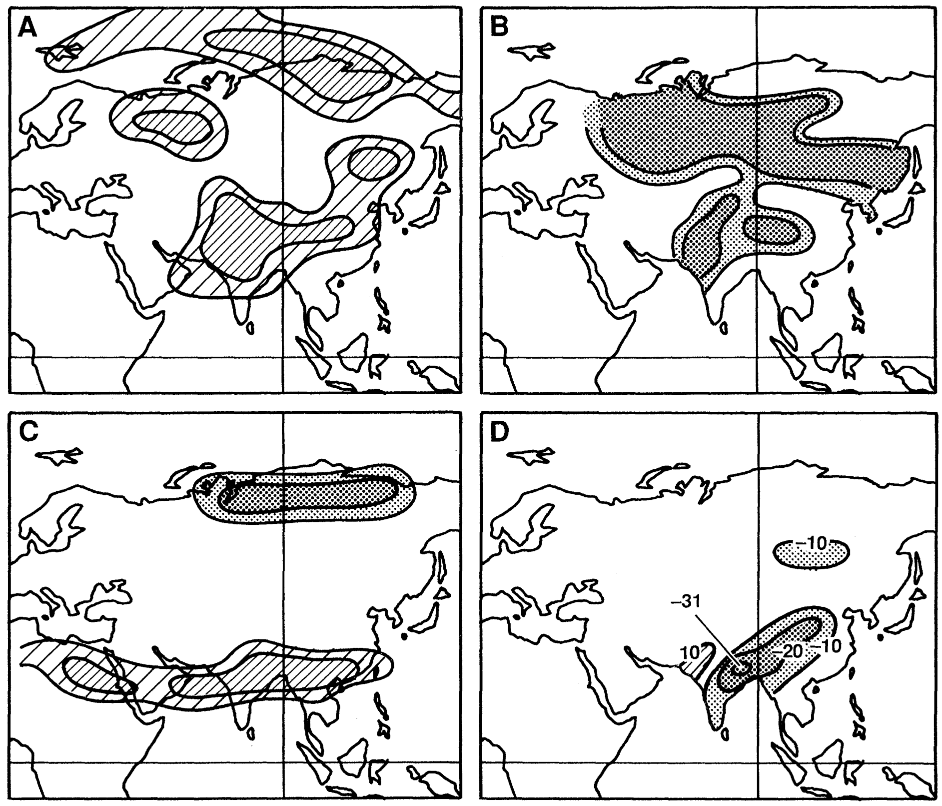

Fig. 1. (**A**) Relative sea level pressure signal over Eurasia in June. The sea level pressure for the control experiment C is subtracted from sea level pressure for the doubled snowfall D experiment. This difference is divided by the standard deviation for the control run. Contour intervals correspond to the 0.10 and 0.05 significance levels. The crosshatch defines positive values of $(D - C)/\sigma$; stipples define negative values. The two densities of hatched and stippled areas correspond to the 0.10 and 0.05 significance levels, respectively. (**B**) Same as (A) except for the June land surface temperature field. The surface temperature is colder in the D experiment. (**C**) Same as (A) except for the zonal wind component (positive for westerlies) at 200 mbar in June. The positive values over India indicated a weakened tropical jet. (**D**) The difference in total precipitation between the doubled snowfall experiment and the control; units are centimeters. The D experiment is characterized by strong reduction in rainfall in the heart of the monsoon region.

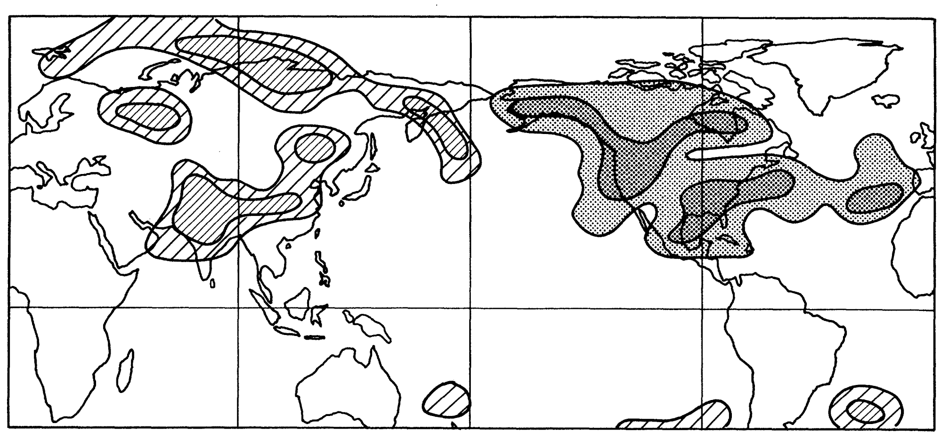

Fig. 2. Sea level pressure in June for the doubled snowfall experiment minus the control divided by standard deviation of the control. See Fig. 1 for meaning of hatching and stippling.

trast that drives the monsoon is dictated by the temperature over the continent, so that during the D experiment the meridional atmospheric temperature gradient over Asia is greatly reduced. Thus, the tropical easterly jet (TEJ) at 200 mbar is weakened by roughly 5 m/sec (20%) (Fig. 1C) and there is also a substantial reduction of the surface wind over the Arabian Sea and in the equatorial Indian Ocean. Observed winds at both the surface and 200 mbar show similar reductions that are in good quantitative agreement with the simulations (*9*). Rainfall is substantially reduced over much of Southeast Asia (Fig. 1D) during D experiments and this represents a huge decrease in the amount of latent heat released to the atmosphere. These results taken together form essentially a classic definition of a "poor" monsoon (*9*). The values shown on the illustration are generally highly statistically significant according to both the *t* test and PPP test. Virtually all of the above effects can be seen in the H experiments but they have the opposite sign (as expected). In other words, the D-H experiments are highly compatible and support the conclusion that variable snow mass over Eurasia affects the subsequent monsoon.

One apparent peculiarity in the results is that during a poor monsoon the model suggests a small increase in precipitation in the region of Pakistan and Afghanistan. This would not normally be expected. However, a separate analysis of the Southeast Asian rainfall field indicates that the opposition of the rainfall anomaly sign between these regions and the rest of Southeast Asia is the second most preferred mode of rainfall variation in this area. Thus, although our model results do differ slightly from the classical definition (*9*) of a poor monsoon, the model produces precipitation patterns that do appear in an analysis of the real rainfall data itself.

The simulations show interesting remote responses, namely, a subsequent reduction in late spring SLP over North America during the D experiments, large changes in the tropical geopotential field, and significant, though short-lived, modification of the Pacific trade wind fields. The teleconnection to North America is manifest most strongly in June as a huge region of lower than normal pressure (−2 to −6 mbar) extending from the eastern Pacific over the continent and into the Atlantic Ocean (Fig. 2). In conjunction with the high pressure (+2 to +8 mbar) over Asia, this pattern represents a major readjustment of atmospheric mass field in the mid- to high latitudes of the Northern Hemisphere. The temporal evolution of this anomaly can be traced from May, when it first appears south of the Aleutians, through August, by which time it has virtually disappeared. Analysis of 34 years of observed SLP data clearly shows the same characteristic pattern as produced by the model: higher than normal pressure over Asia and lower than normal pressure over the eastern Pacific and North America during poor summer monsoons.

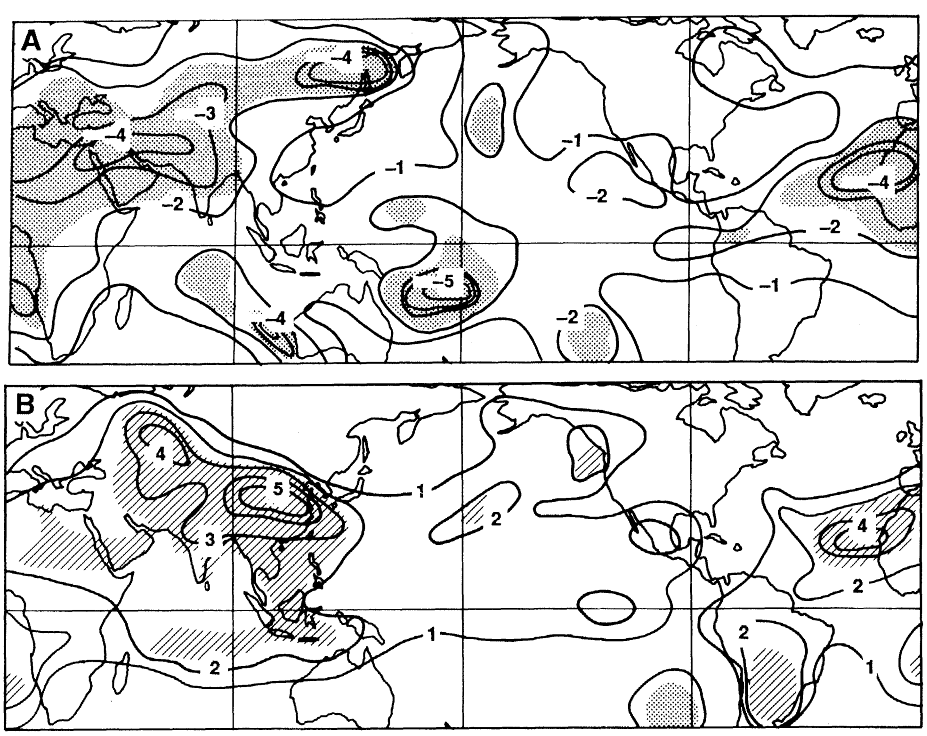

Fig. 3. Typical 200-mbar geopotential height anomaly for the (**A**) D and (**B**) H experiments. See Fig. 1 for meaning of hatching and stippling. Contour intervals are standard deviations.

The anomalies in the 200-mbar height field also show the remote teleconnections from the monsoon are of global dimension and exceptionally strong (Fig. 3). Typical height anomalies correspond to a temperature change of 1° to 2°C. In the tropical strip, the anomalies are coherent around the entire globe. They also bear the expected relation to the monsoon precipitation anomalies; less precipitation during D gives less latent heat release and lower heights and vice versa during H experiments. Note the apparent similarity between these properties of the 200-mbar anomalies from the D-H runs and those observed to occur during the winter season of El Niño–Southern Oscillation (ENSO) events (*10*).

The remotely forced anomalies in the zonal surface wind stress over the equatorial Pacific during the H experiment show a large-scale, statistically significant strengthening in the April-May period. The signal is located mainly in the equatorial zone and deep tropics of the Northern Hemisphere. This is apparently associated with a strengthening of the surface convergence in the western Pacific due to increased precipitation in that area and thus represents a positive feedback. The wind stress anomalies resemble those associated with the cold phase of an ENSO event (*11*). The wind stress over much of the central Pacific in the D experiment is generally decreased in a manner again reminiscent of the windfield during El Niños, but the magnitude of the signal, though significant, is only about half that required to produce a moderate El Niño.

It is perhaps surprising that the main tropical responses obtained in the snow depth experiments bear such a close resemblance to atmospheric anomalies observed during ENSO events. However, qualitative hypotheses have recently been offered to explain the interaction of large-scale atmospheric anomalies over Eurasia and subsequent ENSO development (*2*). Empirical evidence also suggests a close relation between poor monsoon rainfall and near simultaneous occurrence of El Niño, although it is not clear which event occurs first (*12*).

We show elsewhere (*13*) that the surface wind stress perturbations in the D experiments can produce a weak (0.8°C) El Niño in a sophisticated ocean model. Repeating a D experiment with T21 interactively coupled to the same ocean model produced an El Niño of nearly twice the strength (1.5°C). Thus the snowfall perturbations may act as a trigger for some ENSO events. They cannot directly force an ENSO, since their characteristic time scale is about one season, compared to the much longer

ENSO time scale. In summary, the GCM and ocean model results suggest that land processes (anomalous Eurasian snow cover) may play an important role in the ENSO cycle, a role largely unsuspected to date.

Monsoon studies often refer to the role of the Tibetan Plateau as an elevated heat source that forces the reversal of the circulation by season (*14*). The snow perturbation experiments do not confine forcing to the Tibetan area alone, but rather distribute it over a larger part of the Eurasian continent. It is characteristics of this larger scale forcing field that we now discuss. Speculation regarding the mechanisms by which a large-scale snow field might affect the atmosphere (*6, 15–17*) has included the direct effects of the snow cover such as albedo effects, as well as changes in sensible or latent heat flux from the snow-covered land. Analysis of our model simulations, although preliminary, indicates that the response is more complex than offered to date.

The physical mechanisms seem to work in two main stages. When excess snow is present, increased albedo is countered by decreased latent heat loss and there is a small heat gain by the continent. Sensible heat and long-wave radiation are in the same sense so that the land mass acts like a heat sink. However, the land stays colder than normal longer into the seasonal cycle since this small positive net heat flux is used as heat of fusion to melt the snow and so cannot warm the land surface. Once the snow is melted, it adds to the reservoir of ground water that eventually gives up an anomalous amount of moisture (latent heat). Again, additional energy is required, because this reservoir is held at a lower temperature than normal for that time of year and therefore further delays and weakens the large-scale land-sea temperature contrast necessary for the summer monsoon.

One could expect that once the snow cover is gone, its effects would be quickly forgotten by the atmosphere. In pure albedo experiments, our model gave just such results. But the above-mentioned effects, due to the fully interactive hydrological cycle, conspire to negate this conclusion in the perturbation experiments.

Finally, at the second stage, when the snow has disappeared, solar radiation is again important but for a different reason. It is now affected by the increase or decrease of cloud cover associated with an increased or decreased monsoon system and atmospheric moisture content. Latent heat flux is the other dominant term in the surface heat budget as described above. Of the remaining elements of the surface heat budget, long wave radiation from the surface is reduced since the earth is colder than normal under the heavy snowfall regime and sensible heat flux is also reduced.

Surface convergence and diabatic heating over Southeast Asia normally causes strong upward vertical motions of warm air that subsequently descends over other tropical regions of the world. It is thought that this subsidence, fed from the Southeast Asia region, is an important element in the maintenance of the subtropical ridge in the North Pacific during the summer season (*18, 19*). When the Eurasian snow cover is heavier or lighter than usual, the convergence associated with the Southeast Asian monsoon is significantly affected. This modulates the amount of energy and mass that may be transported from the Southeast Asian region to other areas during the monsoon. As a consequence, the tropical atmosphere, for example, 200-mbar height and surface wind fields, would be expected to respond in much the manner found in the simulations.

The causes for the large-scale teleconnection to the North American continent can be understood as the response of the atmosphere to large-scale thermal forcing from the surface of the Asian continent. The necessary readjustment of the atmospheric mass field is carried out by "external" Rossby wave dynamics (*20*).

REFERENCES AND NOTES

1. H. F. Blanford, *Proc. R. Soc. London* **37**, 3 (1984).
2. T. P. Barnett, *J. Atmos. Sci.* **42**, 478 (1985); T. Yasunari, *J. Meteorol. Soc. Jpn.* **65**, 81 (1987).
3. D. G. Hahn and J. Shukla, *J. Atmos. Sci.* **33**, 2461 (1976).
4. B. Dey and O. S. R. U. Bhanu Kumar, *J. Geophys. Res.* **88**, 5471 (1983).
5. R. R. Dickson, *J. Clin. Appl. Meteorol.* **23**, 171 (1984).
6. T.-C. Yeh, R. Wetherald, S. Manabe, *Mon. Weather Rev.* **111**, 1013 (1983).
7. G. Fischer, Ed., *Large-Scale Atmospheric Modelling, Rep. No. 1* (Meteorologishes Institüt, University of Hamburg, Hamburg, 1987).
8. R. Preisendorfer and T. P. Barnett, *J. Atmos. Sci.* **40**, 1884 (1983).
9. H. H. Lamb, *Climate Present, Past, and Future* (Methuen, London, 1973), vol. 1; M. Tanaka, *Climatological Notes 26, Occasional Papers No. 2* (Institute for Geosciences, University of Tsukuba, Tsukuba, Japan, 1980); S. Hastenrath, *Climate Circulation of the Tropics* (Reidel, Dordrecht, 1985); J. Fein and P. Stevens, *Monsoons* (Wiley, New York, 1987).
10. J. Horel and J. Wallace, *Mon. Weather Rev.* **109**, 813 (1981); T. Barnett, *J. Atmos. Sci.* **42**, 2798 (1985).
11. T. P. Barnett, *J. Phys. Oceanog.* 7, 633 (1977); A. J. Busalacchi and J. J. O'Brien, *J. Geophys. Res.* **86**, 901 (1981); *J. Phys. Oceanog.* **10**, 1929 (1980).
12. B. Weare, *J. Atmos. Sci.* **36**, 2279 (1979); J. Angell, *Mon. Weather Rev.* **109**, 230 (1981); E. Rassmusson and T. Carpenter, *ibid.* **111**, 516 (1983).
13. T. P. Barnett, L. Dümenil, M. Latif, U. Schlese, E. Roeckner, unpublished results.
14. J. Flohn, M. Hantel, E. Ruprecht, *Bonner Met. Abhand.* **14**, 1 (1970); J. Charney, *Q. J. Roy. Meteorol. Soc.* **111**, 193 (1975); H. He, J. McGinnis, Z. Song, M. Yanai, *Mon. Weather Rev.* **115**, 1966 (1987).
15. P. B. Wright, *Meteorol. Mag.* **96**, 302 (1967).
16. A. Robock, *J. Atmos. Sci.* **40**, 986 (1983).
17. J. O. Roads, *J. Geophys. Res.* **86**, 7411 (1981).
18. T. N. Krishnamurti, *J. Atmos. Sci.* **28**, 1342 (1971); D. Johnson, R. Townsend, M.-Y. Mei, *Tellus* **37A**, 97 (1985).
19. E. Palmén and C. Newton, *Atmospheric Circulation Systems* (Academic Press, New York, 1969); H. Flohn, *Bonner Met. Abhand.* **15**, 55 (1971).
20. I. Held, *Large-Scale Dynamical Processes in the Atmosphere*, B. Hoskins and R. Pearce, Eds. (Academic Press, New York, 1983), p. 123.

21. Supported by NSF grant ATM85-13713 and by Deutsche Forschungsgemeinschaft through SFB 318 and by Bundesminister für Forschung und Technologie, grant K-F 20128, and the Max-Planck-Institut für Meteorologie, Hamburg. We thank J. Roads and S. Chen for many useful suggestions.

8 September 1987; accepted 14 December 1987